

Antiproton-nucleon annihilations into three pions

T. E. Kalogeropoulos, L. Gray, A. Nandy, and J. Roy*

Department of Physics, Syracuse University, Syracuse, New York 13210

(Received 3 March 1981)

New data are presented for antiproton capture in deuterium for the reactions (a) $\bar{p}d \rightarrow 2\pi^- \pi^+ p_s$ at rest with spectator proton, (b) $\bar{p}d \rightarrow 2\pi^- \pi^+ p_s$ with the antiproton in flight (~ 0.35 GeV/c momentum), and (c) $\bar{p}d \rightarrow 2\pi^- \pi^+ p$ at rest but with nonspectator protons. The striking features of the $2\pi^- \pi^+$ Dalitz plot for (a) are compared with $\bar{p}p \rightarrow 3\pi^0, \pi^+ \pi^- \pi^0$ at rest, with $\bar{p}d \rightarrow 2\pi^- \pi^+ p_s$ at other energies, and with predictions of dual models. No consistent and satisfactory interpretation has been found. The possible quantum numbers of the $2\pi^- \pi^+$ final state are discussed.

I. INTRODUCTION

Nucleon-antinucleon annihilations into three pions have been of considerable interest in the past. The new antiproton facilities under construction are expected to bring them again into focus during this decade. It is the purpose of this paper to bring up to date all the available experimental results in suitable forms for further analyses, point out the lack of any consistent understanding, and raise questions which can be answered by future experiments.

The extended phase space and the existence of four possible 3π charge states naturally suggested them for the investigation of the $\pi\pi$ interaction. These states are

$$\bar{p}n \rightarrow \pi^+ \pi^- \pi^-, \quad (1)$$

$$\bar{p}n \rightarrow \pi^- \pi^0 \pi^0, \quad (2)$$

$$\bar{p}p \rightarrow \pi^0 \pi^0 \pi^0, \quad (3)$$

$$\bar{p}p \rightarrow \pi^+ \pi^- \pi^0. \quad (4)$$

The first three reactions are pure in I -spin ($=1$) while (4) is mixed ($I=0, 1$). Although it is in principle more attractive to study the pure I -spin states, experimentally they are harder to study because they require deuterium or/and $>1 \pi^0$. Consequently the reaction (4) was studied as soon as antiproton beams became available to the bubble chambers at CERN (Refs. 1 and 2) and BNL (Ref. 3) followed with the study of (1) by the Rome-Syracuse collaboration⁴ and later by the study of (3) by the Columbia-Syracuse collaboration.⁵ There are no data on reaction (2).

These studies have been made at rest where additional constraints on the overall quantum numbers were expected to be valid. Based on the theory for nuclear capture from atomic states by Day, Snow, and Sucher,⁶ it was expected that annihilations at rest would occur from S states in liquid H_2 (D_2). Their theory was successful in predicting⁷ π^-, K^-, Σ^- captures, while the early ob-

servation⁸ of a small $\bar{p}p \rightarrow K_S K_S / \bar{p}p \rightarrow K_S K_L$ ratio was considered as confirmation that the $\bar{p}p$ captures as well go via S states. In this case, since $G_{3\pi} = -1 = G_{\bar{N}N} = (-1)^{L+S+I}$, the $I=0, 1$ states are associated with the $^3S_1, ^1S_0$ states, respectively. Zemach⁹ parametrized the 3π amplitudes in terms of the $\pi\pi$ interaction for all possible 3π quantum numbers. It was therefore first hoped that the study of these annihilations at rest would yield the $\pi\pi$ interactions in all I -spin states.

The $\bar{p}p \rightarrow \pi^+ \pi^- \pi^0$ data revealed abundant and equal ρ^+, ρ^-, ρ^0 production superimposed on a uniform background. The equality of ρ^+, ρ^-, ρ^0 production implies via I -spin conservation ($\pi^0 \rho^0$ is forbidden from $I=1$) that the $\rho\pi$ is produced in $I=0$; the uniform background was interpreted¹⁻³ as resulting from $I=1$. The $\bar{p}n \rightarrow \pi^+ \pi^- \pi^-$ data,⁴ however, did not support these conclusions. Instead of an expected uniform Dalitz plot it exhibited spectacular structures. Moreover, as shown in Ref. 4, analysis in terms of the $\pi\pi$ interaction in the manner of Zemach (final-state-interaction model) gave unacceptable solutions, particularly since the fits required an exotic ($I=2$) $\pi\pi$ resonance near threshold. These unphysical results led Lovelace¹⁰ to an application of the Veneziano model¹¹ which was claimed to reproduce the essential features of the $\pi^+ \pi^- \pi^-$ final state without requiring a $\pi^+ \pi^-$ resonance. The apparent success of this model gave great impetus to the study of dual models and several¹²⁻¹⁹ improved ones have been tested claiming better fits to this reaction. The observation of the reaction $\bar{p}p \rightarrow 3\pi^0$ revealed⁵ similarities to $\bar{p}n \rightarrow \pi^+ \pi^- \pi^-$ but was not helpful in understanding the $\pi^+ \pi^- \pi^-$ structures.

The measurement of the $(\bar{p}p \rightarrow 2\pi^0) / (\bar{p}p \rightarrow \pi^+ \pi^-)$ and $(\bar{p}d \rightarrow \pi^- \pi^0 p_s) / (\bar{p}d \rightarrow \pi^+ \pi^- n_s)$ branching ratios at rest in hydrogen^{20,21} and deuterium²² implies that (40-75)% of all $\bar{N}N$ annihilations into 2π go via odd $\bar{N}N$ angular momenta. Further, inclusive tests of I -spin conservation in $\bar{p}d$ annihilations at rest showed large I -spin-violating effects.²³ The consequences of these phenomena to the interpretation of 3π

annihilations are difficult to entertain. For example, in spite of these observations the 3π may still come from S states and conserve I -spin but it cannot be taken for granted. In any case, the sharpness of the structures in $2\pi^-\pi^+$ at rest strongly suggest that it has unique spin, parity, and I -spin.

In Sec. II of this paper all the available data (about twice that first published⁴) on $\bar{p}d \rightarrow \pi^+\pi^-\pi^+p_s$ at rest will be presented in suitable forms for analyses. Also, for the first time data will be presented on this reaction in flight (0.2–0.4 GeV/ c) and at rest with high-momentum (>0.2 GeV/ c) recoiling “spectator” protons. In Sec. III, we compare the reaction $\bar{p}d \rightarrow \pi^+\pi^-\pi^+p_s$ at rest with $\bar{p}p \rightarrow \pi^+\pi^-\pi^0$, $\pi^0\pi^0\pi^0$ as well as with predictions of dual models. Furthermore, we raise questions on the quantum numbers of the $2\pi^-\pi^+$ final states at rest and attempt to get model-independent restrictions on them. In Sec. IV, we summarize our observations and appeal for further experimental and theoretical work.

II. EXPERIMENTAL RESULTS

A. Measurements and analysis

The data presented here on $\bar{p}d$ annihilation into $\pi^+\pi^-\pi^+$ come from an analysis of about 3×10^6 $\bar{p}d$ events. These events have been collected from exposures of the 30-in. bubble chamber filled with deuterium to a stopping antiproton beam produced by the Alternating Gradient Synchrotron at Brookhaven.

The yield per annihilation of events of interest is rather small ($\sim 1\%$). In order to reduce the measurements, events with three prongs which did not show clear momentum imbalance on the scanning table were measured. The momentum-conservation criterion was based only on angles and reduced the measurements of the three-prong events by a factor of 3. Further, it was required that all except stopping tracks have projected lengths in the three views of >5 cm. Measurements were also made on a limited sample without any of these cuts including events with visible protons (four-prong). Comparison of the $\pi^+\pi^-\pi^+$ Dalitz plots for these types of measurements showed no evidence of biases.

The measurements after reconstruction were subjected to kinematical fits assuming no missing neutral particle or one π^0 and zero \bar{p} momentum. The contamination of the $\bar{p}d \rightarrow 2\pi^-\pi^+p$ events by in-flight and/or $1\pi^0$ events has been estimated⁴ to be $\leq 1\%$.

B. Spectator spectrum

Figure 1 shows the momentum distribution obtained by fitting the three- and four-prong events with $2\pi^-\pi^+p$. The spectrum has been fitted with a Fourier transform of the deuteron wave function fudged with the experimental resolution and a Maxwellian distribution $[\propto p^2 \exp(-E/T)]$. Maxwellian distributions fit $\pi^\pm, K^\pm, K^0, \Lambda$ inclusive spectra in $\bar{p}d$ annihilations at rest²⁴ adequately. The nonspectator, Maxwellian contribution amounts to $(25 \pm 2)\%$ and the temperature T is 80 MeV. The extrapolation of the Maxwellian distribution to the three-prong events, which represent the bulk of our measurements, yields a 0.7% contamination by nonspectators.

In order to shed some light into the nature of the nonspectator events, the invariant π^+p mass distributions are presented in Fig. 2 for the events with protons of momentum >0.2 GeV/ c . Proton spectra from $\bar{p}d$ annihilations in flight have been interpreted²⁵ as due to initial- and final-state (πp rescattering) effects. At rest only πp rescattering can affect the proton spectrum. In this case, however, the presence of a strong Δ^{++} is compulsory. The absence of any Δ^{++} evidence suggests that this is not the principal mechanism of the nonspectator protons. We favor an interpretation based on a three-body initial-state mechanism.^{26,27} In either case, these considerations will not affect the conclusions of this paper.

C. $\bar{p}d \rightarrow 2\pi^-\pi^+p$ at rest

The $2\pi^-\pi^+$ Dalitz plot for all events with a spectator proton is shown in Fig. 3. The total number

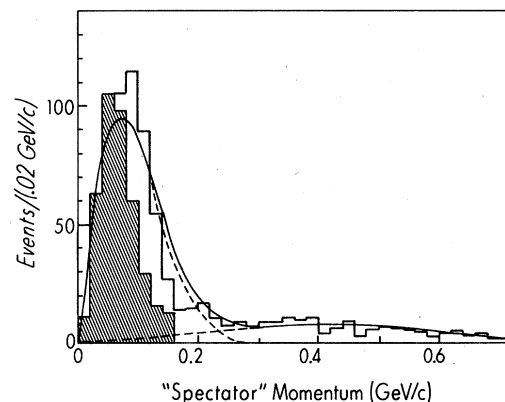


FIG. 1. Proton momentum spectrum in $\bar{p}d \rightarrow 2\pi^-\pi^+p$ at rest. Shaded events are due to three-prong events. Solid line is a fit with the Fourier transform of the deuteron wave function and a Maxwellian distribution. The Maxwellian distribution contributes $(25 \pm 2)\%$ and the temperature is 80 MeV.

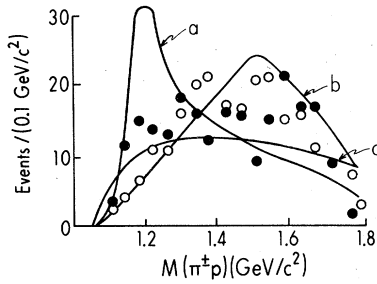


FIG. 2. $M(\pi^\pm p)$ distributions for $\bar{p}d \rightarrow 2\pi^- \pi^+ p$ at rest with $p_p > 0.2$ GeV/c. The $\pi^- p$ scale has been normalized to the $\pi^+ p$. Curves (a) and (b) are predictions of final-state scattering between the pions from annihilation and spectators: (a) for $\pi^+ p$ and (b) for $\pi^- p$. Curve (c) is "phase space" prediction from a three-body initial-state interaction. Open circles $\pi^- p$, closed circles $\pi^+ p$ mass spectra.

of events is 5512 including 2785 from Ref. 4. Its projection on the $\pi^+ \pi^-$, $\pi^- \pi^-$ axes are presented in Figs. 4 and 5. The resolution in $M^2(\pi\pi)$ is ~ 0.05 GeV²/c⁴ over the entire plot. In Fig. 6, in analogy to the $3\pi^0$ data,⁵ the data of Fig. 3 are presented in tabular form for the convenience of those who would like to test other models.

In Fig. 7 the $2\pi^- \pi^+$ Dalitz plot is presented for

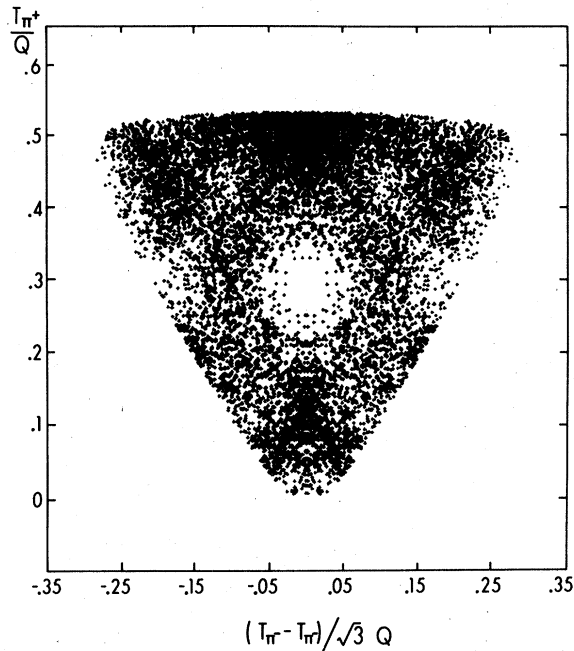


FIG. 3. $2\pi^- \pi^+$ symmetric Dalitz plot for all (5512) $\bar{p}d \rightarrow 2\pi^- \pi^+ p_s$ at-rest events ($Q = 2m_p - 3m_\pi$). There are two points per event corresponding to the interchange of the two negative pions. The hole is at (or near) the center where all pions have equal momenta. At the castle (see text) the negative pions have equal momenta (magnitude and directions).

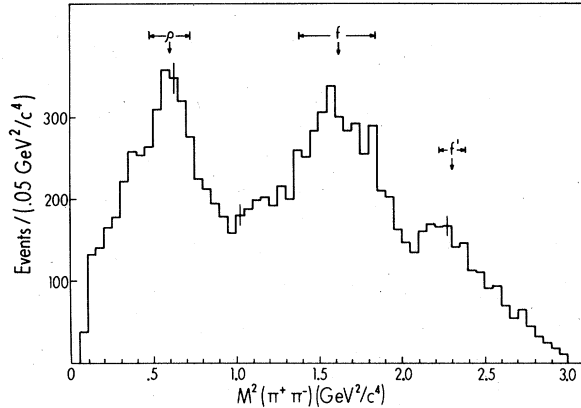


FIG. 4. $M^2(\pi^+ \pi^-)$ distribution of the events in Fig. 3. The positions and widths of the ρ , f , and f' mesons are indicated.

nonspectator events with proton momenta 0.2–0.4 GeV/c while Fig. 8 shows the $M^2(\pi^- \pi^-)$ distribution for those events. The total energy of these events is 32–127 MeV below the $\bar{N}N$ threshold and, as indicated, the boundary is not well defined.

D. $\bar{p}d \rightarrow 2\pi^- \pi^+ p_s$ in flight

We have identified among our three-prong measurements the $2\pi^- \pi^+$ events from annihilations in flight. In the fiducial region about 20% of all annihilations are expected to occur in flight with \bar{p} momentum of ≤ 0.45 GeV/c. Their identification has been made as follows.

The events which did not fit as either $2\pi^- \pi^+$ or $2\pi^- \pi^+ \pi^0$ at rest have been considered as in-flight candidates. The in-flight $2\pi^- \pi^+ p_s$ events are expected to (a) yield a missing mass squared (MM^2) $\approx -|\vec{p}_F|^2$, (b) have a measured momentum (\vec{p}_{meas}) in the direction of the beam, and (c) have a total energy $\approx (2m_p + 0.02$ GeV). In Fig. 9 the distribu-

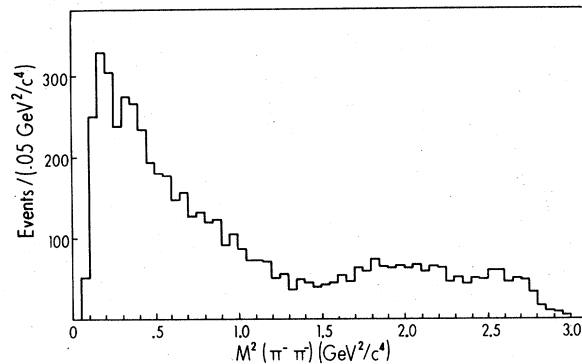


FIG. 5. $M^2(\pi^- \pi^-)$ distribution of the events in Fig. 3. The enhancement starting at threshold is related to the castle (see text) or the f peak of Fig. 4.

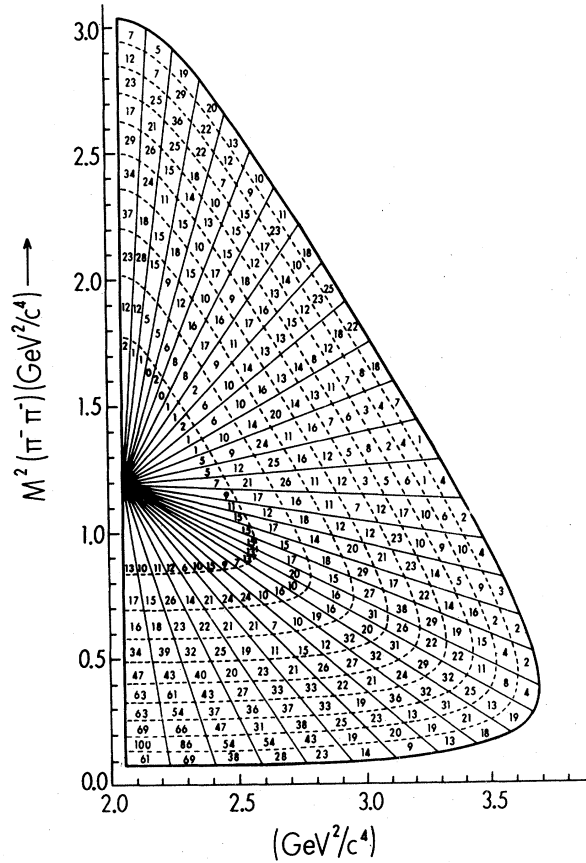


FIG. 6. Event distribution within the $2\pi^-\pi^+$ symmetric Dalitz plot. Radial-azimuthal cells have same areas. Note that the density over the plot varies by at least two orders of magnitude.

tion of the events as a function of the measured energy squared is shown for those candidates with $MM^2 < -0.02 \text{ GeV}^2/c^4$, $|\vec{p}_{\text{meas}}|^2 > 0.03 \text{ GeV}^2/c^4$, and an angle between \vec{p}_{meas} and beam of $< 30^\circ$. The clear peak in Fig. 9 at the right energy for in-flight events is absent (Fig. 10) for events which

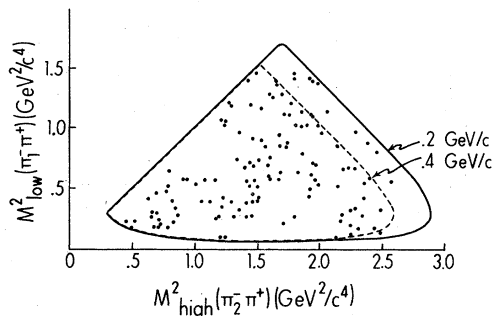


FIG. 7. $2\pi^-\pi^+$ Dalitz plot for $\bar{p}d \rightarrow 2\pi^-\pi^+p$ at rest for nonspectator protons with a momentum between 0.2 and 0.4 GeV/c .

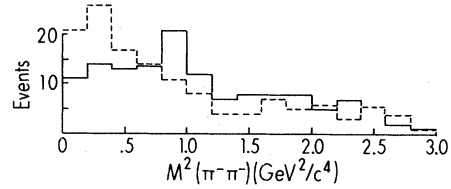


FIG. 8. $M^2(\pi^-\pi^+)$ distribution for the events in Fig. 7. Dashed histogram is expected distribution from Fig. 5. The castle effect seems to be absent in the nonspectator events.

have an angle between \vec{p}_{meas} and the beam $> 30^\circ$. The distribution of the events with measured energy squared ($3-4 \text{ GeV}^2$) (Fig. 9) as a function of $|\vec{p}_{\text{meas}}|$ is shown in Fig. 11. Since the maximum \vec{p} momentum is $\sim 0.45 \text{ GeV}/c$, a cut has been made at this value.

In Fig. 12 the $2\pi^-\pi^+$ Dalitz plot for these in-flight events is shown in comparison with an equal sample of $2\pi^-\pi^+$ at rest. The boundary of the in-flight Dalitz plot at high masses is not well defined because of the spread in beam momentum. Their projections on the $M^2(\pi^+\pi^-)$, $M^2(\pi^-\pi^+)$ axes are presented in Fig. 13.

From the limited measurements in which the beam and both three- and four-prong $\bar{p}n$ events were measured, we have extracted a small sample of $2\pi^-\pi^+p_s$ in-flight events by performing kinematical fits including both beam and spectator. Figure 14 shows the distribution of these events as a function of \vec{p} momentum and Fig. 15 shows their distribution in terms of the angle of the normal to the $2\pi^-\pi^+$ plane (in its c.m. system) with the beam.

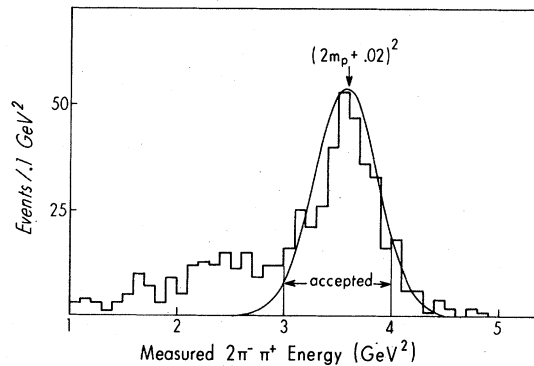


FIG. 9. Distribution of events, which did not fit to either $2\pi^-\pi^+(p_s)$ or $2\pi^-\pi^+\pi^0(p)$ rest, and which has forward ($< 30^\circ$) measured $2\pi^-\pi^+$ momentum and negative missing mass, as a function of the $2\pi^-\pi^+$ measured energy squared.

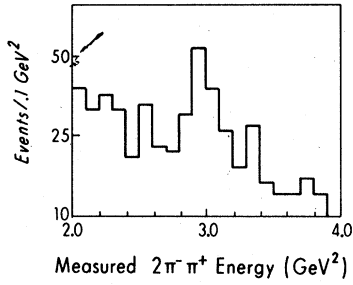


FIG. 10. Same as in Fig. 9 except that measured momentum made an angle to the beam $>30^\circ$.

E. Branching ratios

1. $\bar{p}d \rightarrow 2\pi^-\pi^+p_s$ at rest

Branching ratios have been obtained from 52706 $\bar{p}d$ events in which each event was classified either as $\bar{p}n$ or $\bar{p}p$ and the topology and kaons were recorded. 1684 events had kaons. The event was measured only if the tracks (π^+) had projected lengths >5 cm. About 25% of the three- and four-prong events were unmeasurable and 18% failed to be reconstructed. We have evaluated the $2\pi^-\pi^+p_s$ branching ratio at rest as follows:

$$f^R(2\pi^-\pi^+p_s) \equiv \frac{(2\pi^-\pi^+p_s)^R}{(\text{all } p_s)^R} = \frac{(\text{three prongs})^R}{(\text{odd prongs})^R} \times \frac{(2\pi^-\pi^+p_s)^R}{(\text{three prongs})^R}, \quad (5a)$$

where R refers to at-rest events. The ratio of three-prong to odd-prong events is 0.59 and is independent of energy. We identified 438 $2\pi^-\pi^+p_s$ among the 10522 analyzed three-prong events involving ~ 8733 at rest. It was found by Monte Carlo simulation that 19% of the $2\pi^-\pi^+p_s$ events are rejected by the projected length criterion while the rejection rate for $2\pi^-\pi^+\pi^0p_s$ is only 9%. This has

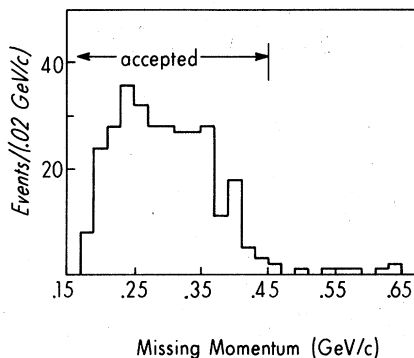


FIG. 11. Distribution of accepted events (Fig. 9) versus $2\pi^-\pi^+$ measured momentum. The accepted events in this figure are assumed to be in-flight $2\pi^-\pi^+p_s$ events.

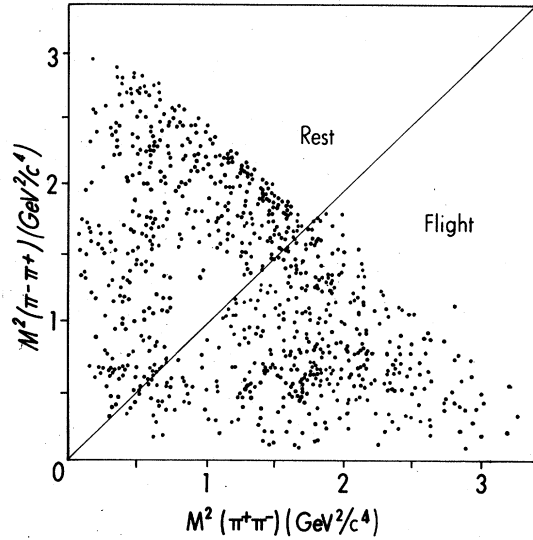


FIG. 12. Dalitz plot of the $\bar{p}d \rightarrow 2\pi^-\pi^+(p_s)$ in flight compared with an equal but random sample of the at-rest events. The hole among the in-flight events has disappeared.

been confirmed from the angular distribution of the normal to the $2\pi^-\pi^+$ c.m.-system plane with the optic axis which showed a 16% rejection. Using these factors we get

$$f^R(2\pi^-\pi^+p_s) = 0.59 \times \frac{438 \times 1.16}{8733} = (3.4 \pm 0.2)\%, \quad (5b)$$

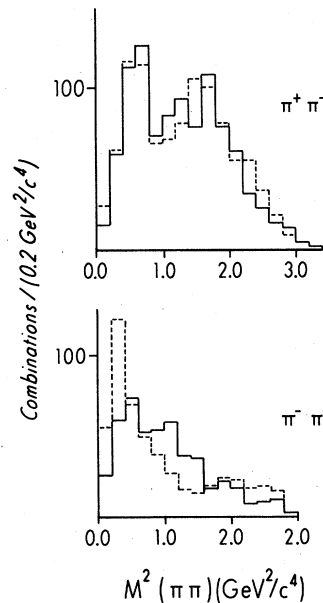


FIG. 13. Comparison of the in-flight (solid) and at-rest (dashed) $M^2(\pi\pi)$ distributions. Note that the castle, showing as an enhancement at low-mass $\pi^-\pi^-$ mass, is absent among the in-flight events.

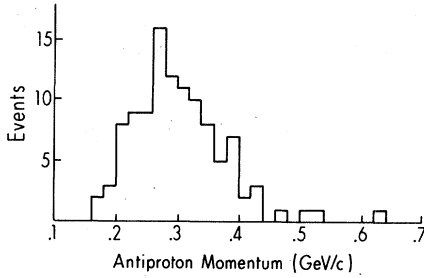


FIG. 14. Distribution of $\bar{p}d \rightarrow 2\pi^- \pi^+ p_s$ in-flight events as a function of the \bar{p} momentum obtained kinematically.

the error being statistical. This result is higher than the one of Ref. 4 $[(2.4 \pm 0.4)\%]$ reflecting our corrections due to measuring biases and in-flight contamination.

2. $\bar{p}d \rightarrow 2\pi^- \pi^+ p_s$ in flight

In the same measurements (IID and Figs. 14 and 15) 125 $2\pi^- \pi^+ p_s$ in-flight events were identified. Thus

$$(2\pi^- \pi^+ p_s)^F / (2\pi^- \pi^+ p_s)^R = 0.20 \pm 0.02. \quad (6)$$

Using $\bar{p}d$ cross sections $\sim 20\%$ of the annihilations in the fiducial region are expected to be in flight. Consequently, there is no evidence for variation of the $2\pi^- \pi^+ p_s$ branching ratio from at-rest to in-flight captures.

III. DISCUSSION

A. Features of 3π annihilations

1. $\bar{p}d \rightarrow 2\pi^- \pi^+ p_s$ at rest

The most important features of the $2\pi^- \pi^+$ final state can be seen in Fig. 3 and they have been pointed out in Ref. 4. For convenience in discussing them they will be identified as follows.

“Hole”. Absence of events near or at the 3π symmetry point $[M^2(\pi^+ \pi_1^-) = M^2(\pi^+ \pi_2^-) \simeq 1 \text{ GeV}^2/c^4]$.

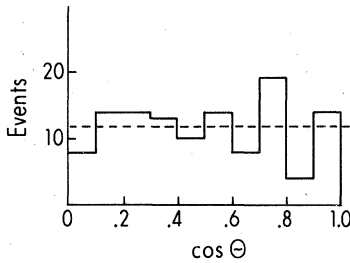


FIG. 15. Angular distribution of the events in Fig. 14. θ is the angle between the normal to the $2\pi^- \pi^+$ plane (in their c.m. system) and the \bar{p} momentum. Dashed line represents isotropy.

“Castle”. Principal enhancement centered at $M^2(\pi^+ \pi_1^-) \simeq M^2(\pi^+ \pi_2^-) = m_f^2 \simeq 1.6 \text{ GeV}^2/c^4$. The relative density in the castle region to that in the hole (see Fig. 6) is greater than $\sim 100:1$.

“Tower A”. An enhancement centered at $M^2(\pi^+ \pi_1^-) \simeq M^2(\pi^+ \pi_2^-) = m_\rho^2 \simeq 0.5 \text{ GeV}^2/c^4$.

“Tower B”. An enhancement at $M^2(\pi^+ \pi_1^-) \simeq m_\rho^2$, $M^2(\pi^+ \pi_2^-) = m_f^2 = 2.3 \text{ GeV}^2/c^4$.

The $M^2(\pi\pi)$ distributions (Figs. 4 and 5) are reflections of these important features. The castle is responsible for the f peak (Fig. 4) and the enhancement at low $\pi^- \pi^-$ mass (Fig. 5). The towers are responsible for the peaks at the ρ and f' masses. The ρ and f peaks have also been enhanced by the hole which is half way between the ρ and f peaks.

Other suppressions and enhancements are also evident. For example, there is suppression at $M^2(\pi^+ \pi_{1,2}^-) = 2$ and $M^2(\pi^+ \pi_{2,1}^-) = 0, 1 \text{ GeV}^2/c^4$. Further, a narrow peak is suggested near the Dalitz-plot boundary and within the castle.

Variations of the density of events along various strips and around interesting points are shown in Figs. 16 and 17. The castle, hole, and tower A

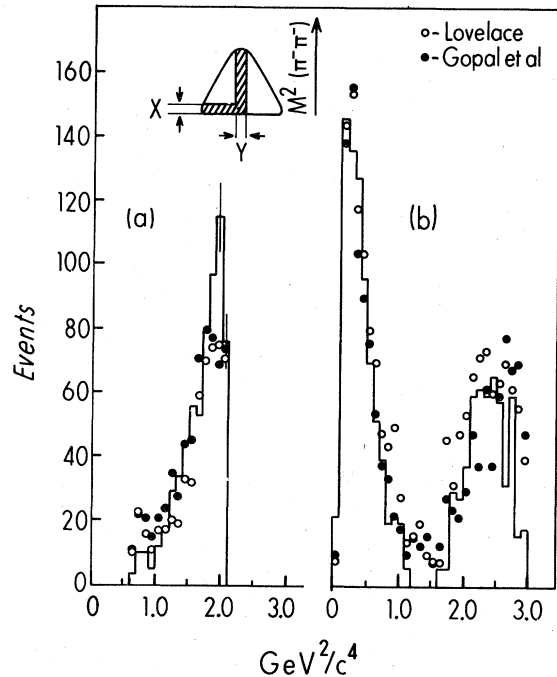


FIG. 16. Distribution of the $2\pi^- \pi^+$ at-rest events along (a) the X strip or $M^2(\pi^- \pi^-) = \text{constant}$, (b) the Y strip or $M^2(\pi^- \pi^-)$ decreasing. The large peaks are due to the castle while the smaller one in (b) is due to tower A. The data are compared with the dual models using parameters obtained by Lovelace and Gopal *et al.* In (a) a narrow peak within the castle is suggested as a $\sim 4\sigma$ effect.

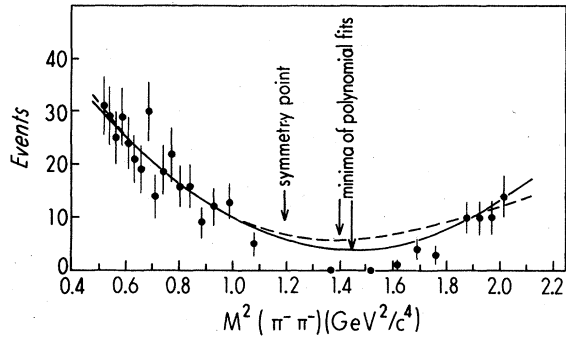


FIG. 17. Same as in Fig. 16(b) emphasizing the region around the hole. Curves are fits to two polynomials.

effects, and their relative densities are well seen in Fig. 16(b). The narrow peak within the castle is shown in Fig. 16(a) as a $\sim 4\sigma$ effect.

2. $2\pi^-\pi^+$ versus $\pi^+\pi^-\pi^0$ and $3\pi^0$ at rest

In Fig. 18 our $2\pi^-\pi^+$ data at rest are compared with the CERN-College de France² $\pi^+\pi^-\pi^0$ at-rest data. In contrast to the $2\pi^-\pi^+$ the $\pi^+\pi^-\pi^0$ Dalitz plot is structureless, except for the uniform and equal intensity ρ^+ , ρ^- , ρ^0 bands. In particular, there is no evidence for the hole or the castle, which are the most impressive features of the $2\pi^-\pi^+$ Dalitz plot.

The equality of the ρ^+ , ρ^- , ρ^0 production in $\bar{p}p$

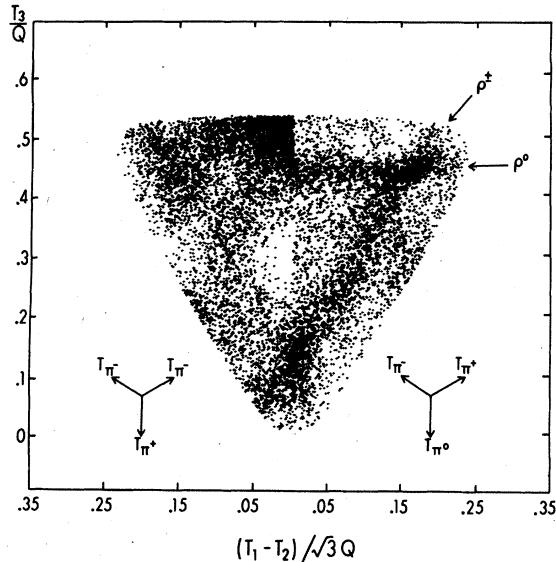


FIG. 18. Comparison of the $2\pi^-\pi^+$ at-rest (left half) with the $\pi^+\pi^-\pi^0$ (right half) at-rest data from Ref. 2. The $\pi^+\pi^-\pi^0$ does not show any evidence for either the castle or the hole effects.

implies that the reaction $\bar{N}N \rightarrow \rho\pi$ is produced from the $I=0$ initial states. This is consistent with the conclusion of Ref. 4 that in spite of the impressive " ρ peak" (Fig. 4), due primarily to the tower A and hole, it does not fit with a $\rho^0\pi^-$ amplitude. The suppression of the $\rho\pi$ from $I=1$ is surprising because if one assumes that the 3π comes from S states then all kinematical variables, including internal relative angular momenta, are the same for both I -spins.

In Fig. 19 the $2\pi^-\pi^+$ data are compared with the Columbia-Syracuse⁵ $3\pi^0$ data. Since these two reactions come from $I=1$ $\bar{N}N$ states one hopes to identify some common features. Indeed, and as already pointed out,⁵ the castle and hole are present in the $3\pi^0$ but not as impressively.

3. $2\pi^-\pi^+$ versus center-of-mass energy

It is interesting to explore the dependence of $2\pi^-\pi^+$ main features as a function of energy below and above the $\bar{N}N$ threshold. If the strong features are associated with initial-state phenomena they would depend on energy while if they are consequences of $\pi\pi$ interactions then slow variations with energy are expected.

The in-flight events presented in Fig. 12 represent the smallest energy change from at rest (see Fig. 11). Another sample has been studied by the Melbourne group²⁸ at \bar{p} incident momenta ~ 0.40 to 0.92 GeV/c. Bettini *et al.*²⁹ studied this reaction at ~ 1.2 GeV/c and Susinno *et al.*³⁰ at ~ 3.0 GeV/c.

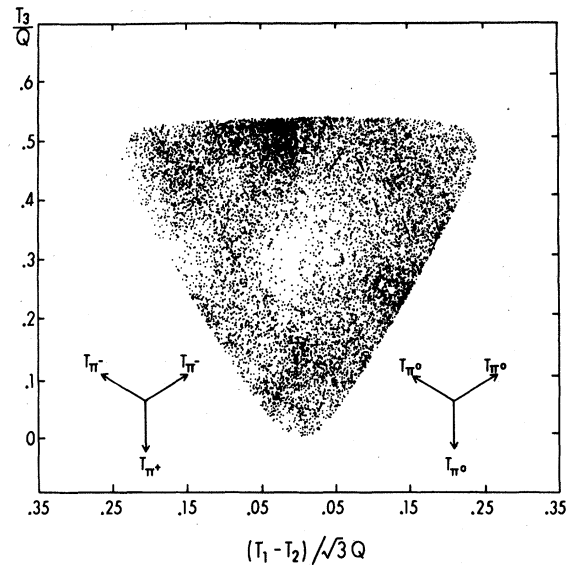


FIG. 19. Comparison of the $2\pi^-\pi^+$ at-rest (left half) with the $3\pi^0$ (right half) at-rest data from Ref. 5. The $3\pi^0$ show some evidence for the castle and hole.

The striking features of our in-flight data are the absences of the hole and the castle structures which are evident in Figs. 12 and 13. One may argue that the emergence of $L_{\bar{N}N} > 0$ waves are responsible for these qualitative changes. The angular distribution (Fig. 15), however, does not support such an assumption. Similar conclusions, particularly the absence of the hole, have been reached by the Melbourne group. Although not as pronounced as at rest, Bettini *et al.* see the dual-model regularities (holes-enhancements) including the at-rest hole. Susinno *et al.* at much higher energies observe more or less a structureless Dalitz plot. The Dalitz plots of all presently available $2\pi^-\pi^+$ data as a function of antiproton momentum are presented in Fig. 20 for comparison.

The annihilations at rest in deuterium, even with a spectator of zero momentum, are below the $\bar{p}n$ threshold. Owing to the binding of nucleons, these annihilations are a few MeV below threshold and by taking into account the spread in spectator energy the data on $\bar{p}n \rightarrow 2\pi^-\pi^+$ at rest have a spread of a few MeV in total energy. To study this reaction, or any other, much lower in energy one has to use³¹ higher-energy spectators but it is not clear then how to select these events because of initial ($\bar{p}n$) and final (πN) effects.²⁵ At any rate, the data in Fig. 7 give a first look on the behavior of the main features of the $2\pi^-\pi^+$ at energies below (32–127 MeV) threshold. Within the limited statistics and the spread in the position of the symmetry point over the events, the hole seems to be present. However, the castle as seen in the $M^2(\pi^-\pi^+)$ distribution (Fig. 8) has definitely disappeared. Note that the low $\pi\pi$ mass spectra are insensitive to the variations in total energy.

B. Comparisons with models

Many attempts have been made in the past in order to understand the features of the annihilations at rest into three pions. These attempts fall into two categories: final-state-interaction and dual models.

1. Final-state-interaction models

The interactions of the particles are complicated and any simple approach can only hope to get broad agreements.³² Nevertheless, this has been the standard approach³³ in analyzing three-body final states. In this model the amplitude is expressed as a superposition of two particle resonances and a structureless background. This model was applied^{2,3} to the $\bar{p}p \rightarrow \pi^+\pi^-\pi^0$ and, due to its simple structure (Fig. 18), the model was successful in the interpretation of the data. The

application⁴ of this model, however, to the $\bar{p}n \rightarrow 2\pi^-\pi^+$ at rest failed notably. In particular, it was found necessary to introduce an $I=2$ (exotic) $\pi\pi$ resonance at threshold to account for the castle and even then the fit to the data was marginal. A modified Breit-Wigner amplitude used by Gleeson *et al.*³⁴ using 14 parameters again gave marginal fits.

2. Dual models

The gross failure of the final-state-interaction model to describe the $2\pi^-\pi^+$ data at rest led Lovelace¹⁰ to an application of the dual-model amplitudes¹¹ that seemed to describe these data successfully without introducing exotics. The amplitude which was used is

$$A(s, t) \propto \frac{\Gamma(1 - \alpha_s)\Gamma(1 - \alpha_t)}{\Gamma(2 - \alpha_s - \alpha_t)}, \quad (7)$$

where s, t are $M^2(\pi^+\pi_{1,2}^-)$ and $M^2(\pi^+\pi_{2,1}^-)$, respectively. α_s and α_t are the known Regge-trajectory parameters. For example,

$$\alpha_s = 0.483 + 0.0885s + 10.28(s/4m_\pi^2)^{1/2}. \quad (8)$$

This amplitude generates peaks and valleys at the singularities of the Γ functions (see Fig. 21) and in particular predicts peaks at the castle and tower A, and a suppression at the hole. This initial qualitative success led to increased efforts in understanding the details. Altarelli and Rubinstein¹² pointed out the deficiencies in the one-term dual amplitude and constructed a more general amplitude by adding "satellite" terms. They fitted the projections (Figs. 4 and 5) of the Dalitz plot and defined a three-term amplitude which was later¹³ justified by considering factorization of the five-point function. A more general approach based on five-point functions was made by Bender and Rothe.¹⁴ Many other attempts¹⁵⁻¹⁷ were made without improved results. The best fit to the data has been made by Gopal *et al.*¹⁸ They were the first to fit the Dalitz plot instead of the projections in which many details were washed out. They used the Altarelli-Rubinstein amplitude and by careful consideration of the coefficients and of the imaginary part of the ρ trajectory succeeded in getting the best fit so far to the data.

It may be useful to illustrate the kind of fits that these models achieve by comparing the data with the Lovelace and Gopal *et al.* amplitudes. Using their parameters and Monte Carlo techniques as many $2\pi^-\pi^+$ events were generated as the data and are compared vis a vis in Figs. 22 and 23 and Fig. 16. Neither fit reproduces the depth of the hole and other details.

The qualitative interpretation of the most prominent features of the data by the dual models is

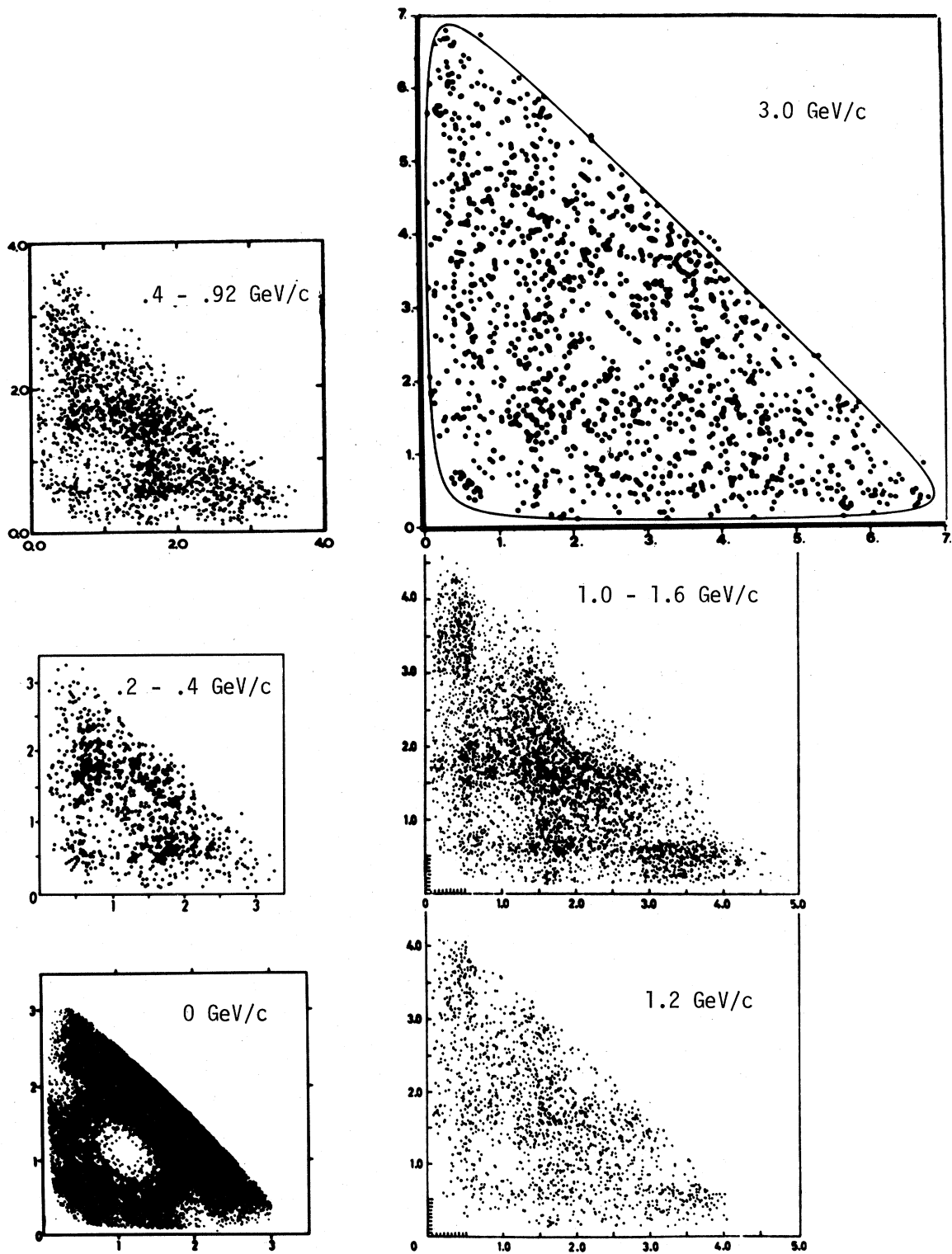


FIG. 20. Comparison of all available $\bar{p}d \rightarrow 2\pi^- \pi^+ p_s$ Dalitz plots as a function of energy. At-rest and 0.2–0.4 GeV/c data, this work; 0.42–0.92 GeV/c, Ref. 28; 1.2 GeV/c and 1.0–1.6 GeV/c, Ref. 29; 3.0 GeV/c, Ref. 30. Note the sharp structures of the at-rest data are unique. The region 1.0–1.6 GeV/c shows dual-model-like regularities.

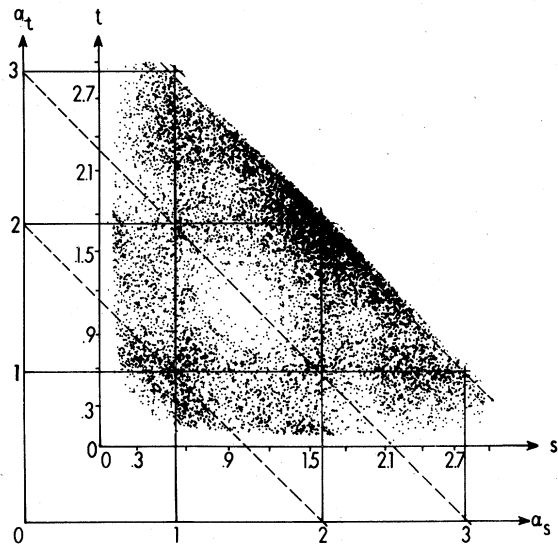


FIG. 21. The $2\pi^-\pi^+$ at-rest Dalitz plot compared with dual amplitudes. The solid lines correspond to the maxima of the Γ functions at the numerator of the Eq. (7) while the dashed ones correspond to the maxima of the Γ function at the denominator. The castle, hole, and tower A are consistent with such an amplitude but not tower B.

indeed remarkable. However, since these models depend on s and t , they will fail in interpreting our in-flight $2\pi^-\pi^+$ data (Fig. 12). Further they fail badly when applied to the $\bar{p}p \rightarrow 3\pi^0$ data (Fig. 24).

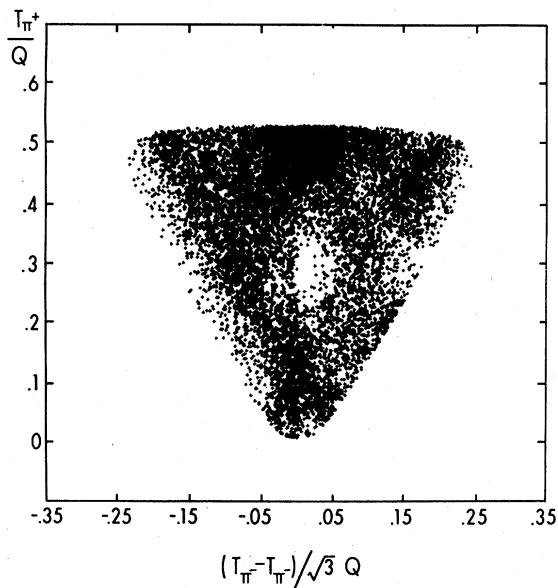


FIG. 22. Comparison of the $2\pi^-\pi^+$ at-rest Dalitz plot according to Lovelace (left half) with the data (right half).

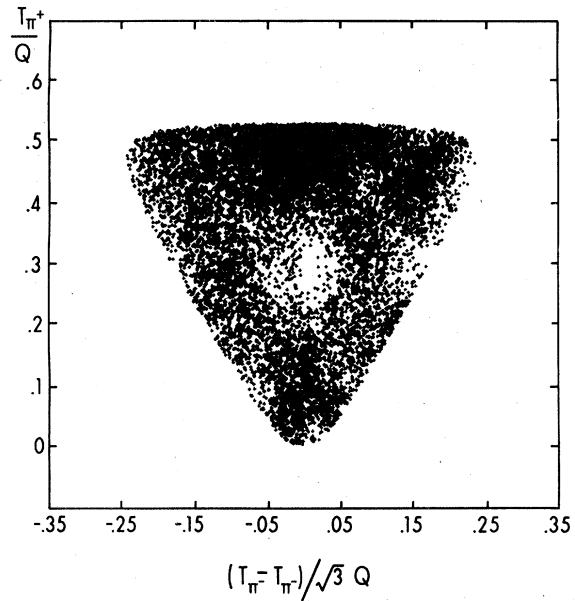


FIG. 23. Comparison of the $2\pi^-\pi^+$ at-rest Dalitz plot according to Gopal *et al.* (left half) with the data (right half).

C. $2\pi^-\pi^+$ quantum numbers

The intriguing $2\pi^-\pi^+$ at-rest Dalitz plot for which no satisfactory interpretation has yet been found, the observations on 2π annihilations²⁰⁻²² in regard to S capture, and the I -spin-violating neutral excess²³ invite the following questions.

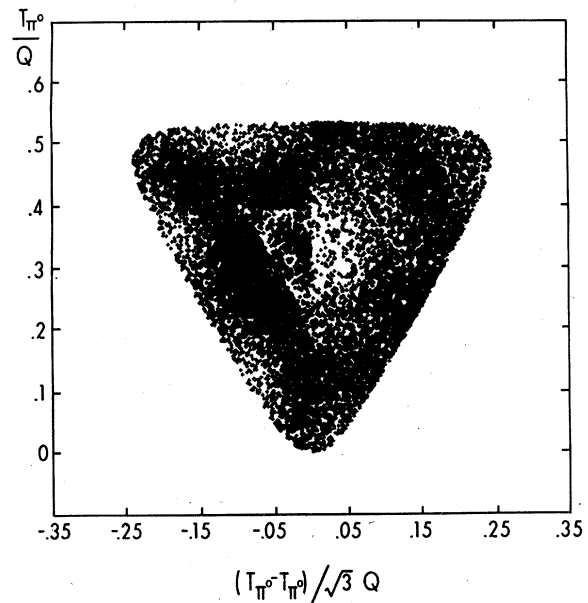


FIG. 24. Comparison of the $3\pi^0$ at-rest Dalitz plot according to Lovelace (left half) with the data of Devons *et al.* (right half).

1. Do the $2\pi^-\pi^+$ come from S states?

It was generally believed on good theoretical and experimental grounds that the capture of anti-protons at rest proceed via S Bohr states until the observation of the 2π by Devons *et al.*²⁰ confirmed recently by Dalpiaz *et al.*²¹ Gray *et al.*,²² by measuring the $\pi^-\pi^0/\pi^+\pi^-$ in deuterium, reached similar conclusions. Thus, on the basis of the 2π annihilations, there is no evidence in H_2 or D_2 that the annihilations proceed via S states. However, the annihilations⁸ into $K^0\bar{K}^0$ are in agreement with the S capture hypothesis. These observations on channels with branching ratios of $\sim(1-3)\times 10^{-3}$ cannot be extrapolated to the total or to other channels. Therefore, the question of the capture leading to any channel is open. We would like to argue here that the $2\pi^-\pi^+$ Dalitz plot is not inconsistent with S capture.

The sharp features of the Dalitz plot and in particular the hole make very probable the hypothesis that they belong to definite quantum numbers. Comparison of the data (Fig. 3) with the zeros of the matrix elements implied by the symmetry⁹ excludes $J^P=1^-, 2^+, 3^-$. These J^P states have zeros all along the boundary and there is no such evidence in the data. Further, $J^P=1^+, 3^+$ imply zero for zero π^+ kinetic energy and this is not supported by the data. Thus, independent of isospin considerations, the only possible J^P assignments are $0^-, 2^-$, etc. The $\bar{p}p$ intrinsic relative parity has been confirmed³⁵ to be negative and thus we conclude that the only possible $\bar{p}n$ states are $^1S_0, ^1D_2, \dots$

2. Is the hole a consequence of symmetry suppression?

The depth and the proximity of the hole to the symmetry point raises the question of whether it may be due to symmetries. The only possible 3π state that can produce a zero at the center of the Dalitz plot is $I, J^P=2, 0^-$. It is therefore important to locate the exact position of the minimum to eliminate such a possibility. In Fig. 17 an attempt is made to identify the position of the minimum independently of specific models. Although it seems that the minima of the polynomial fits are outside the symmetry point, we believe that on the basis of statistics, diffusion of the symmetry point due to the spectator, and the uncer-

tainties in the parametrization of the density it is premature to exclude the possibility that the minimum coincides with the symmetry point.

IV. SUMMARY AND CONCLUSIONS

The $2\pi^-\pi^+$ Dalitz plot from $\bar{p}d$ at-rest annihilations is revisited with almost twice the original events. They are presented in convenient forms that allow independent studies. The striking hole-enhancement structures originally seen have been further enhanced and new "microstructures" are emerging requiring more data on this channel.

We have looked at the dependence of the most pronounced features (hole and castle) of the $2\pi^-\pi^+$ Dalitz plot at rest as a function of the $2\pi^-\pi^+$ mass and in other charged states ($3\pi^0, \pi^+\pi^-\pi^0$). For the first time, data on this channel above and below threshold are presented. These data and other data at higher energies show that the hole and castle are principally characteristic of the at-rest annihilations. The $3\pi^0$ at rest seem to have these structures, although less pronounced, but not the $\pi^+\pi^-\pi^0$.

Final-state-interaction models require an unacceptable $I=2$ $\pi\pi$ resonance near the 2π threshold. Dual models of Lovelace and others appear to have the right structure for the hole and castle but they fail in getting the depth of the hole and making overall good fits. Further, they do not consistently fit at other energies and other channels ($3\pi^0, \pi^+\pi^-\pi^0$). We thus conclude that there is no satisfactory and consistent model describing $\bar{N}N \rightarrow 3\pi$.

Based on general symmetry principles we conclude that $J^P=0^-$ or 2^- , etc., for the $2\pi^-\pi^+$ at rest. Further, if the hole is interpreted as the result of symmetries then $J^P=0^-$ and $I=2$. If this were true then the "minimum" of the hole has to coincide with the symmetry point. The present data do not exclude this possibility.

Further experimental and theoretical studies of 3π annihilations, particularly around threshold, are imperative in order to understand these intriguing features of the $2\pi^-\pi^+$ annihilations at the $\bar{N}N$ threshold.

ACKNOWLEDGMENT

This work has been supported by The National Science Foundation, Washington, D.C.

*Permanent address: Jadavpur University, Calcutta, India.

¹G. B. Chadwick, W. T. Davies, M. Derrick, C. J. B. Hawkins, T. H. Mulvey, D. Radojicic, C. A. Wilkinson,

M. Cresti, S. Limentani, and R. Santangelo, Phys. Rev. Lett. **10**, 62 (1963).

²M. Foster, Ph. Gavillet, G. Labrosse, L. Montanet, R. A. Salmeron, P. Villemoes, C. Ghesquière, and

- L. Lillestøl, Nucl. Phys. **B6**, 107 (1968).
- ³C. Baltay, P. Franzini, N. Gelfand, G. Ludjens, J. Sevens, J. Steinberger, D. Tycko, and D. Zanello, Phys. Rev. **140**, B1039 (1965).
- ⁴P. Anninos, L. Gray, P. Hagerty, T. Kalogeropoulos, S. Zenone, R. Bizzarri, M. Gaspero, I. Laakso, S. Lichtman, and G. C. Moneti, Phys. Rev. Lett. **20**, 402 (1968).
- ⁵S. Devons, T. Kozlowski, P. Némethy, S. Shapiro, M. Dris, N. Horwitz, T. Kalogeropoulos, J. Skelly, R. Smith, and H. Uto, Phys. Lett. **47B**, 271 (1973).
- ⁶T. B. Day, G. A. Snow, and J. Sucher, Phys. Rev. Lett. **3**, 61 (1959); B. Desai, Phys. Rev. **119**, 1385 (1960).
- ⁷For π^- see T. H. Fields *et al.*, Phys. Rev. Lett. **5**, 61 (1959); J. H. Doede *et al.*, Phys. Rev. **129**, 2808 (1963); E. Bierman *et al.*, Phys. Lett. **4**, 351 (1963). For K^- see R. Knop *et al.*, Phys. Rev. Lett. **14**, 767 (1965); M. Cresti *et al.*, *ibid.* **14**, 487 (1965). For Σ^- see R. A. Burnstein *et al.*, Phys. Lett. **17**, 344 (1965).
- ⁸C. Baltay *et al.*, Phys. Rev. Lett. **15**, 639 (1965); **15**, 597(E) (1965).
- ⁹Ch. Zemach, Phys. Rev. **133**, B1201 (1964).
- ¹⁰C. Lovelace, Phys. Lett. **28B**, 264 (1968).
- ¹¹G. Veneziano, Nuovo Cimento **47A**, 642 (1967).
- ¹²G. Altarelli and H. R. Rubinstein, Phys. Rev. **183**, 1469 (1969).
- ¹³H. R. Rubinstein, E. J. Squires, and M. Chaichian, Phys. Rev. Lett. **30B**, 189 (1969).
- ¹⁴I. Bender and H. J. Rothe, Z. Phys. **247**, 186 (1971).
- ¹⁵C. Boldrighini and A. Pugliese, Lett. Nuovo Cimento **2**, 239 (1969).
- ¹⁶S. Pokorski, R. O. Raitio, and B. H. Thomas, Nuovo Cimento **7A**, 828 (1972).
- ¹⁷R. Odorico, Phys. Lett. **33B**, 489 (1970); G. Franzen and H. Romer, Lett. Nuovo Cimento **5**, 689 (1972).
- ¹⁸G. P. Gopal, R. Migneron, and A. Rothary, Phys. Rev. D **3**, 2262 (1971).
- ¹⁹A. Nandy, P. H. Frampton, and T. E. Kalogeropoulos, Phys. Rev. D **11**, 1040 (1975).
- ²⁰S. Devons, T. Kozlowski, P. Némethy, S. Shapiro, N. Horwitz, T. Kalogeropoulos, J. Skelly, R. Smith, and H. Uto, Phys. Rev. Lett. **27**, 1614 (1971).
- ²¹G. Bassompierre, G. Binder, P. Dalpiaz, P. F. Dalpiaz, G. Gissinger, S. Jacquen, G. Maderni, C. Peroni, M. A. Schneegans, and L. Techio, in *Proceedings of the IV European Antiproton Symposium*, Barr, edited by A. Fridman (Editions du Centre National de la Recherche Scientifique, Paris, 1979), Vol. 1, p. 139.
- ²²L. Gray, Th. Papadopoulou, E. Simopoulou, A. Vayaki, T. Kalogeropoulos, and J. Roy, Phys. Rev. Lett. **30**, 1091 (1973).
- ²³T. E. Kalogeropoulos, T. A. Filippas, G. Grammatikakis, Th. Papadopoulou, E. Simopoulou, A. Vayaki, L. Gray, J. Roy, and G. Tzanakos, Phys. Rev. Lett. **33**, 163 (1974); **33**, 1635 (1974).
- ²⁴J. Roy, in *Proceedings of the Fourth International Symposium on NN Interactions, Syracuse, New York, 1975*, edited by T. E. Kalogeropoulos and K. C. Wali (Syracuse University, Syracuse, 1975), Vol. 1, p. III-1.
- ²⁵P. D. Zeman, Z. Ming Ma, and J. M. Mountz, Phys. Rev. Lett. **38**, 1443 (1977).
- ²⁶R. Bizzarri, G. Ciapetti, U. Dore, E. C. Fowler, P. Guidoni, I. Laakso, F. Marzano, G. C. Moneti, D. Zanello, L. Gray, P. Hagerty, T. Kalogeropoulos, and S. Zenonne, Lett. Nuovo Cimento **2**, 431 (1969).
- ²⁷T. E. Kalogeropoulos and G. S. Tzanakos, in *Antinucleon-Nucleon Interactions*, proceedings of the Stockholm Symposium, 1976, edited by G. Ekspong and S. Nilsson (Pergamon, New York, 1977), p. 29.
- ²⁸S. N. Tovey, K. R. Parker, G. Chapman, J. De Roach, E. Gold, D. Kasper, P. A. King, A. G. Klein, L. J. Martin, G. C. Mason, G. I. Opat, and J. W. G. Wignall, Phys. Rev. D **17**, 2206 (1978).
- ²⁹A. Bettini, M. Cresti, M. Mazzucato, L. Peruzo, S. Sartori, G. Zumerle, M. Alson-Garnjost, R. Husman, R. Ross, F. T. Solmitz, L. Bertanza, R. Carrara, Casali, P. Lariccia, R. Pazzi, G. Borreani, B. Quasiasi, G. Rinando, M. Vigone, and A. Werbroock, Nuovo Cimento **1A**, 333 (1971).
- ³⁰G. Susinno, L. Votano, A. Bettini, M. Cresti, M. Mazzucato, L. Peruzo, P. Rossi, G. Sartori, S. M. Sartori, L. Ventura, G. Zumerle, L. Barone, R. Bizzarri, G. Ciapetti, C. Dionisi, P. F. Lovere, V. Rossi, E. Valente, E. Castelli, C. Omero, P. Poropat, and M. Sessa, in *Antinucleon-Nucleon Interactions* (Ref. 27), p. 197.
- ³¹T. E. Kalogeropoulos and G. S. Tzanakos, Phys. Rev. Lett. **34**, 1047 (1975).
- ³²This was pointed out in the case of an exactly soluble three-body weak decay by R. A. Amado and J. V. Noble, Phys. Rev. **185**, 1993 (1963) and also by D. Sivers, Phys. Rev. D **5**, 2392 (1972).
- ³³The final-state-interaction model was first formulated by K. M. Watson, Phys. Rev. **88**, 1163 (1952) and applied to $\bar{N}N$ annihilations by C. Bouchiat and G. Flammang, Nuovo Cimento **23**, 13 (1962).
- ³⁴A. M. Gleeson, W. J. Meggs, and M. Parkinson, Phys. Rev. Lett. **25**, 74 (1970).
- ³⁵T. E. Kalogeropoulos, C. B. Chiu, and E. C. G. Sudarshan, Phys. Rev. Lett. **37**, 1037 (1976). E. Okonov and M. Shirokov, Phys. Lett. **68B**, 88 (1977).